

# A Three-Step Approach for Assessing Landscape Connectivity via Simulated Dispersal: African Wild Dog Case Study

David D. Hofmann<sup>1,2,§</sup>  Gabriele Cozzi<sup>1,2</sup>  John W. McNutt<sup>2</sup>  
Arpat Ozgul<sup>1</sup>  Dominik M. Behr<sup>1,2</sup> 

December 13, 2022

<sup>1</sup> Department of Evolutionary Biology and Environmental Studies, University of Zurich,  
Winterthurerstrasse 190, 8057 Zurich, Switzerland.

<sup>2</sup> Botswana Predator Conservation Program, Wild Entrust, Private Bag 13, Maun,  
Botswana.

§ Corresponding author (david.hofmann2@uzh.ch)

**Running Title:** Simulating Wild Dog Dispersal Trajectories to Assess Landscape  
Connectivity

**Keywords:** dispersal, simulation, movement, integrated step-selection function,  
Kavango-Zambezi Transfrontier Conservation Area, landscape connectivity, *Lycaon pictus*

## Abstract

**Context** Dispersal of individuals contributes to long-term population persistence, yet requires a sufficient degree of landscape connectivity. To date, connectivity has mainly been investigated using least-cost analysis and circuit theory, two methods that make assumptions that are hardly applicable to dispersal. While these assumptions can be relaxed by explicitly simulating dispersal trajectories across the landscape, a unified approach for such simulations is lacking.

**Objectives** Here, we propose and apply a simple three-step approach to simulate dispersal and to assess connectivity using empirical GPS movement data and a set of habitat covariates.

**Methods** In step one of the proposed approach, we use integrated step-selection functions to fit a mechanistic movement model describing habitat and movement preferences of dispersing individuals. In step two, we apply the parameterized model to simulate dispersal across the study area. In step three, we derive three complementary connectivity maps; a heatmap highlighting frequently traversed areas, a betweenness map pinpointing dispersal corridors, and a map of inter-patch connectivity indicating the presence and intensity of functional links between habitat patches. We demonstrate the applicability of the proposed three-step approach in a case study in which we use GPS data collected on dispersing African wild dogs (*Lycaon pictus*) inhabiting northern Botswana.

**Results** Using step-selection functions we successfully parametrized a detailed dispersal model that described dispersing individuals' habitat and movement preferences, as well as potential interactions among the two. The model substantially outperformed a model that omitted such interactions and enabled us to simulate 80,000 dispersal trajectories across the study area.

**Conclusion** By explicitly simulating dispersal trajectories, our approach not only requires fewer unrealistic assumptions about dispersal, but also permits the calculation of multiple connectivity metrics that together provide a comprehensive view of landscape connectivity. In our case study, the three derived connectivity maps revealed several wild dog dispersal hotspots and corridors across the extent of our study area. Each map highlighted a different aspect of landscape connectivity, thus emphasizing their complementary nature. Overall, our case study demonstrates that a simulation-based approach offers a simple yet powerful alternative to traditional connectivity modeling techniques. It is therefore useful for a variety of applications in ecological, evolutionary, and conservation research.

# **1 Introduction**

2 Dispersal of individuals is a vital process that allows species to maintain genetic diversity  
3 (Perrin and Mazalov, 2000; Frankham et al., 2002; Leigh et al., 2012; Baguette et al., 2013;  
4 LaPoint et al., 2013), rescue non-viable populations (Brown and Kodric-Brown, 1977), and  
5 to colonize unoccupied habitats (Hanski, 1999; MacArthur and Wilson, 2001). However, the  
6 ability to disperse depends on a sufficient degree of landscape connectivity (Fahrig, 2003;  
7 Clobert et al., 2012), making the identification and protection of dispersal corridors that  
8 promote connectivity a task of fundamental importance (Doerr et al., 2011; Rudnick et al.,  
9 2012). Identifying dispersal corridors not only necessitates a comprehensive understanding  
10 of the factors that limit dispersal, but also an appropriate model to estimate connectivity  
11 (Baguette et al., 2013; Vasudev et al., 2015; Hofmann et al., 2021a). To date, the most  
12 commonly used connectivity models are least-cost path analysis (LCPA; Adriaensen et al.,  
13 2003) and circuit theory (CT; McRae, 2006; McRae et al., 2008). Unfortunately, both models  
14 rest on assumptions that appear unsuitable for dispersers, thus calling for the development  
15 of alternative approaches. One promising alternative is to assess landscape connectivity via  
16 simulated dispersal trajectories generated from individual-based movement models (IBMMs,  
17 Diniz et al., 2019). However, IBMMs require a large number of subjective modeling decisions,  
18 thus making among-system comparisons difficult.

19 Traditional connectivity models make assumptions that are rarely met for dispersers.  
20 LCPA, for instance, assumes that individuals move towards a preconceived endpoint and  
21 choose a cost-minimizing route accordingly (Sawyer et al., 2011; Abrahms et al., 2017).  
22 While this assumption may be justifiable for migrating animals, it is unlikely to hold for  
23 dispersers, as dispersers typically move across unfamiliar territory towards an unknown end-  
24 point (Koen et al., 2014; Cozzi et al., 2020). CT, on the contrary, posits that animals move  
25 according to a random walk, entailing that autocorrelation between subsequent movements  
26 cannot be rendered (Diniz et al., 2019). For dispersers, however, autocorrelated movements  
27 are regularly observed (Cozzi et al., 2020; Hofmann et al., 2021a), meaning that dispersal  
28 trajectories are usually strongly directional. An interesting generalization that bridges the  
29 continuum between LCPA and CT has been proposed by (Panzacchi et al., 2016) and enables  
30 to capitalize on the merits of both approaches. Despite these and several other generaliza-  
31 tions of LCPA and CT (e.g. Pinto and Keitt, 2009; Landguth et al., 2012; Panzacchi et al.,  
32 2016; Brennan et al., 2020), some shortcomings remain. Most notably, all of these methods  
33 rely on static permeability or resistance surfaces that can't reflect the temporal dimension of  
34 dispersal. This permits statements about the expected duration for moving between habitat

35 patches (Martensen et al., 2017; Diniz et al., 2019).

36 The shortcomings inherent to LCPA and CT can be overcome by simulating dispersal  
37 using IBMMs and by converting simulated trajectories into meaningful measures of connec-  
38 tivity (Diniz et al., 2019). In contrast to LCPA and CT, IBMMs allow to explicitly simulate  
39 how individuals move across and interact with the encountered landscape (Kanagaraj et al.,  
40 2013; Clark et al., 2015; Allen et al., 2016; Hauenstein et al., 2019; Zeller et al., 2020), as  
41 well as to render potential interactions between movement behavior and habitat conditions  
42 (Avgar et al., 2016). This shifts the focus towards a more functional view on connectivity  
43 (Tischendorf and Fahrig, 2000). Furthermore, IBMMs generate movement sequentially, i.e.  
44 they generate a series of steps, so that the temporal dimension of dispersal becomes explicit  
45 and allows modeling autocorrelation between successive steps (Diniz et al., 2019). Finally,  
46 simulations from IBMMs do not enforce movement or connections towards preconceived  
47 endpoints but allow individuals to adjust their route “on the go”, thereby preventing biases  
48 arising from misplaced endpoints. Despite these advantages, a unifying approach to simu-  
49 late dispersal and assess connectivity using IBMMs is lacking. Considering the large number  
50 of subjective decisions entailed by IBMMs, an approach that streamlines and standardizes  
51 the application of dispersal simulations to assess connectivity will, however, be critical to  
52 safeguard comparability among studies.

53 Here, we propose and exemplify a simple three-step approach for simulating dispersal and  
54 assessing landscape connectivity (Figure 1). In step one, we combine GPS movement data  
55 of dispersing individuals with habitat covariates to fit a mechanistic movement model via in-  
56 tegrated step-selection functions (ISSFs, Avgar et al., 2016). We chose to use ISSFs because  
57 the framework not only allows inference on the study species’ habitat kernel (i.e. its habi-  
58 tat preferences), but also its movement kernel (i.e. its movement preferences/capabilities)  
59 and potential interactions among the two (Avgar et al., 2016; Fieberg et al., 2021). In  
60 step two, we use the parametrized movement model to simulate dispersal across the study  
61 area. Comparable simulations have already been applied to estimate steady-state utilization  
62 distributions of resident individuals (Potts et al., 2013; Signer et al., 2017) and to model  
63 landscape connectivity, yet disregarding interdependencies between habitat and movement  
64 kernels (Clark et al., 2015; Zeller et al., 2020). Finally, in step three, we convert the simulated  
65 trajectories into three complementary connectivity maps; (i) a heatmap revealing frequently  
66 traversed areas (e.g. Hauenstein et al., 2019; Zeller et al., 2020), (ii) a betweenness-map  
67 delineating dispersal corridors and bottlenecks (e.g. Bastille-Rousseau et al., 2018), (iii) and  
68 a map of inter-patch connectivity, depicting the presence and intensity of functional links

69 between habitat patches, as well as the average dispersal duration required to realize those  
70 connections (e.g. Gustafson and Gardner, 1996; Kanagaraj et al., 2013).

71 We showcase the application of the proposed approach using GPS movement data col-  
72 lected on dispersing African wild dogs (*Lycaon pictus*). The African wild dog is a highly  
73 mobile species whose population persistence heavily relies on the availability of large, natural  
74 or semi-natural landscapes and a sufficient degree of connectivity among remaining subpop-  
75 ulations. Once common throughout sub-Saharan Africa, this species has disappeared from  
76 much of its historic range, largely due to human persecution, habitat fragmentation, and  
77 disease outbreaks (Woodroffe and Sillero-Zubiri, 2012). Wild dogs typically disperse in  
78 single-sex coalitions (McNutt, 1996; Behr et al., 2020) and are capable of dispersing several  
79 hundred kilometers (Davies-Mostert et al., 2012; Masenga et al., 2016; Cozzi et al., 2020).  
80 Although previous studies have investigated connectivity for this species using LCPA (Hof-  
81 mann et al., 2021a) and CT (Brennan et al., 2020), a more comprehensive and mechanistic  
82 understanding of dispersal and connectivity is missing (but see Creel et al., 2020). Nev-  
83 ertheless, with about 6,000 free-ranging wild dogs remaining in fragmented subpopulations  
84 (Woodroffe and Sillero-Zubiri, 2012), reliable information on dispersal behavior and land-  
85 scape connectivity is essential for the conservation of this endangered carnivore. We antic-  
86 ipated that a connectivity assessment based upon our three-step approach would overcome  
87 several of the conceptual shortcomings of traditional connectivity models, while providing  
88 a more detailed view on movement behavior during dispersal its implications for landscape  
89 connectivity.

## 90 **2 Methods**

### 91 **2.1 Case Study**

#### 92 **2.1.1 GPS Data**

93 We applied the three step approach presented in Figure 1 to GPS movement data from  
94 16 dispersing African wild dog coalitions (7 female and 9 male coalitions). This data has  
95 been collected between 2011 and 2019 from a free-ranging wild dog population in northern  
96 Botswana. During dispersal, GPS collars recorded a fix every 4 hours and regularly trans-  
97 mitted data over the Iridium satellite system. To ensure comparable time intervals between  
98 GPS fixes, we removed any fixes that were not successfully obtained at the desired 4-hour  
99 schedule (allowing for a tolerance of  $\pm$  15 minutes). To prepare the data for step-selection  
100 analysis, we converted the fixes ( $n = 4'169$ ) into steps, where each step represented the

101 straight-line movement between two consecutive GPS fixes (Turchin, 1998). We only con-  
102 sidered steps with equal step-durations (i.e. 4 hours) for further analysis. We will refer to  
103 these steps as “realized steps”. We did not differentiate between sexes, for previous research  
104 found little differences between sexes during dispersal (Woodroffe et al., 2019; Cozzi et al.,  
105 2020). Additional details on the data collection and preparation can be found in Cozzi et al.  
106 (2020) and Hofmann et al. (2021a).

### 107 **2.1.2 Study Area**

108 Our simulation of dispersal trajectories and assessment of connectivity spanned across the  
109 entire Kavango-Zambezi Transfrontier Conservation Area (KAZA-TFCA, Figure 2a and b)  
110 and encompassed a rectangular extent of roughly 1.3 Mio. km<sup>2</sup>. With an area of 520'000  
111 km<sup>2</sup>, the KAZA-TFCA is the world’s largest transboundary conservation area and comprises  
112 parts of Angola, Botswana, Namibia, Zimbabwe, and Zambia, thus hosting a rich diversity  
113 of landscapes, ranging from savannah to grassland and from dry to moist woodland habitats.  
114 In its center lies the Okavango Delta, a dominant hydro-geographical feature and the world’s  
115 largest flood-pulsing inland delta. Large portions of the KAZA-TFCA are formally protected  
116 in the form of national parks (NPs) or other protected areas, yet a considerable portion of  
117 the landscape remains human-dominated (e.g. roads, agricultural sites, and settlements).

### 118 **2.1.3 Habitat Covariates**

119 We represented the physical landscape in our study area by the habitat covariates `water-`  
120 `cover`, `distance-to-water`, `woodland-cover`, `shrub/grassland-cover`, and `human-influence`. To  
121 render the seasonal dynamics of water-cover for the extent of the Okavango Delta, we  
122 applied an algorithm that enabled us to obtain weekly updated raster-layers for `water-`  
123 `cover` and `distance-to-water` from MODIS satellite imagery (Wolski et al., 2017; Hofmann  
124 et al., 2021a). This algorithm is now implemented in the `floodmapr` package (available on  
125 GitHub; <https://github.com/DavidDHofmann/floodmapr>). To ensure a consistent resolu-  
126 tion across habitat covariates, we coarsened or interpolated all layers to a resolution of 250  
127 m x 250 m. A detailed description of how we prepared each habitat covariate is provided in  
128 Hofmann et al. (2021a).

129 We performed all data preparations, spatial computations, and statistical analysis in  
130 R, version 4.2.2 (R Core Team, 2022). Some helper functions were written in C++ and  
131 imported into R using the Rcpp package (Eddelbuettel and François, 2011; Eddelbuettel,  
132 2013; Eddelbuettel and Balamuta, 2018).

133 **2.2 Step 1 - Movement Model**

134 We combined the collected GPS data with habitat covariates and used ISSFs (Avgar et al.,  
135 2016) to parametrize a mechanistic movement model. More specifically, we paired each  
136 realized step with a set of 24 randomly generated alternative steps. A realized and its 24  
137 random steps together formed a stratum that received a unique identifier. As suggested by  
138 Avgar et al. (2016), we generated random steps by sampling random turning angles from a  
139 uniform distribution  $(-\pi, +\pi)$  and step lengths from a gamma distribution that was fitted  
140 to realized steps (scale  $\theta = 6'308$  and shape  $k = 0.37$ ). Note that our approach of sampling  
141 turning angles from a uniform distribution does not imply that we assume uniform turning  
142 angles, as we will account for directionality later in the model (Avgar et al., 2016; Fieberg  
143 et al., 2021).

144 Along each realized and random step, we extracted values from underlying habitat covari-  
145 ate layers and we computed averages of each covariate along the steps. Besides extracting  
146 *habitat covariates*, we also computed movement metrics that we used as *movement covari-  
147 ates* in the ISSF models (Avgar et al., 2016; Fieberg et al., 2021). Specifically, we computed  
148 the step length (`sl`), its natural logarithm (`log(sl)`), and the cosine of the relative turning  
149 angle (`cos(ta)`), which is a measure of directionality (Turchin, 1998), for each step. Because  
150 wild dog activity is low during the hot midday hours (Cozzi et al., 2012), we additionally  
151 created the variable `LowActivity`, indicating whether a step was realized during periods of  
152 low wild dog activity (09:00 to 17:00 local time) or high wild dog activity (17:00 to 09:00  
153 local time). To facilitate model convergence, we standardized all continuous covariates to  
154 a mean of zero and a standard deviation of one. Correlations among covariates were low  
155 ( $|r| < 0.6$ ; Latham et al., 2011), so we retained all of them for modeling.

156 To contrast realized steps (scored 1) and random steps (scored 0), we assumed that  
157 animals assigned a selection score  $w(x)$  to each step (Equation 1; Fortin et al., 2005), where  
158  $w(x)$  depended on the step's associated covariates  $(x_1, x_2, \dots, x_n)$  and on the animal's relative  
159 selection strengths (Avgar et al., 2017) towards these covariates  $(\beta_1, \beta_2, \dots, \beta_n)$ :

$$w(x) = \exp(\beta_1 x_1 + \beta_2 x_2 + \dots + \beta_n x_n) \quad (\text{Equation 1})$$

160 The probability of a step  $i$  being realized was then contingent on the step's selection score,  
161 as well as on the selection scores of all other step in the same stratum:

$$P(Y_i = 1 | Y_1 + Y_2 + \dots + Y_i = 1) = \frac{w(x_i)}{w(x_1) + w(x_2) + \dots + w(x_i)} \quad (\text{Equation 2})$$

162 To estimate relative selection strengths (i.e. the  $\beta$ -coefficients), we used mixed effects  
163 conditional logistic regression analysis, implemented through the r-package `glmmTMB` (Brooks  
164 et al., 2017). The implementation of conditional logistic regression has been proposed by  
165 Muff et al. (2020) and allows to model random slopes. The method requires to fix the vari-  
166 ance of the stratum specific intercept to a large value, so we fixed it to an arbitrary high  
167 value of  $10^6$  and used disperser identity to model random slopes for all covariates.

168 Our movement model was based on a habitat selection model that was previously devel-  
169 oped for dispersing wild dogs (hereafter referred to as *base model*, Hofmann et al., 2021a).  
170 In the base model, no interactions among habitat covariates and movement covariates were  
171 considered, so we here expanded the model and allowed for such interactions, acknowledging  
172 that movement preferences during dispersal could depend on habitat conditions (details in  
173 Appendix A1). To determine the most parsimonious movement model among model can-  
174 didates, we ran stepwise forward model selection based on Akaike's Information Criterion  
175 (AIC, Burnham and Anderson, 2002). More specifically, we started with the base model  
176 and iteratively increased model complexity by adding all possible interactions between move-  
177 ment and habitat covariates. Given that the focus of our analysis lied on predicting dispersal  
178 patterns and all model candidates were biologically intuitive, we deemed the use of model  
179 selection appropriate. However, caution should be employed if causal relationships are of  
180 interest, as model selection may lead to biased parameter estimate (Whittingham et al.,  
181 2006). We validated the predictive power of the most parsimonious model using k-fold  
182 cross-validation for case-control studies as described in Fortin et al. (2009). This valida-  
183 tion attests significant prediction ability to the movement model if the model outperforms a  
184 random guess and systematically assigns low ranks (high selection scores) to observed steps  
185 (details in Appendix A2).

### 186 2.3 Step 2 - Dispersal Simulation

187 We used the most parsimonious movement model to simulate individual dispersal trajectories  
188 across the study area. The simulation of a dispersal trajectory resembled an “inverted”  
189 ISSF and was set up as follows. (1) We defined a source point and assumed a random initial  
190 orientation of the simulated animal. (2) Starting from the source point, we generated 25  
191 random steps by sampling turning angles from a uniform distribution  $(-\pi, +\pi)$  and step  
192 lengths from our fitted gamma distribution. (3) Along each random step, we extracted and  
193 averaged values from the habitat covariate layers and we computed the movement metrics  
194  $sl$ ,  $\log(sl)$ , and  $\cos(ta)$ . To ensure compatible scales with the fitted movement model, we

195 standardized covariate values using means and standard deviations from the empirical data.  
196 (4) We applied the parametrized movement model to predict the selection score  $w(x)$  for each  
197 step using Equation 1 and we converted predicted scores into probabilities using Equation 2.  
198 (5) We randomly sampled one of the generated random steps based on assigned probabilities  
199 and determined the animal's new position. We repeated steps (2) to (5) until 2,000 steps  
200 were realized and we repeated the simulation until a total of 80'000 dispersal trajectories  
201 was reached.

202 As source points for the simulations, we distributed 50,000 points at random locations  
203 inside protected areas that were large enough to host an average size wild dog home range  
204 (i.e. > 700 km<sup>2</sup>; Pomilia et al., 2015). We placed another 30,000 points randomly inside the  
205 buffer zone, mimicking potential immigration into the study area (Figure S1).

206 To mitigate edge effects and to deal with random steps leaving the study area, we followed  
207 Koen et al. (2010) and artificially expanded all covariate layers by a 100 km wide buffer  
208 zone. Within the buffer zone, we randomized covariate values by resampling values from the  
209 original covariate layers. Through this buffer zone, simulated dispersers were able to leave  
210 and re-enter the main study area. In cases where random steps crossed the outer border of  
211 this buffer zone, we resampled steps until they fully lied within the buffer zone, essentially  
212 forcing simulated individuals to remain within the expanded study area.

213 To ensure reliable connectivity estimates, we determined the number of simulated dis-  
214 persal trajectories required to reach a “steady state”. For this purpose, we distributed 1,000  
215 rectangular “checkpoints”, each with an arbitrary extent of 5 km x 5 km, at random co-  
216 ordinates within the study area (excluding the buffer). We then determined the relative  
217 frequency at which each checkpoint was traversed by simulated dispersal trajectories (here-  
218 after referred to as relative traversal frequency) as we gradually increased the number of  
219 simulated trajectories from 1 to 50,000. To assess variability in the relative traversal fre-  
220 quency, we repeatedly subsampled 100 times from all 50'000 trajectories and computed the  
221 mean traversal frequency across replicates, as well as its 95% prediction-interval for each  
222 checkpoint. We considered connectivity to have reached a steady state once the width of  
223 the prediction-interval dropped below a value of 0.01 for all checkpoints.

## 224 **2.4 Step 3 - Connectivity Maps**

### 225 **2.4.1 Heatmap**

226 To identify dispersal hotspots within the study area, we created a heatmap indicating the  
227 absolute frequency at which different areas were traversed by simulated dispersal trajectories

(e.g. Hauenstein et al., 2019; Zeller et al., 2020). Specifically, we rasterized all simulated trajectories onto a raster with 1 km x 1 km resolution and tallied resulting layers into a single map. This procedure ensured that every trajectory was only counted once, even if it traversed the same raster-cell multiple times, thus reducing potential biases caused by individuals that were surrounded by unfavorable habitat and “moved in circles”. To achieve high performance rasterization, we used the R-package `terra` (Hijmans, 2021). For a subset of the study area, we also generated heatmaps at 250 m x 250 m, yet found little qualitative differences to the coarser resolution, thus suggesting the choice of 1 km x 1 km to be appropriate.

#### 2.4.2 Betweenness Map

To pinpoint movement corridors and bottlenecks, we converted simulated trajectories into a network and calculated betweenness scores for all raster-cells in the study area (Bastille-Rousseau et al., 2018). Betweenness is a pertinent metric for connectivity as it measures how often a specific network-node (in our case a raster-cell) lies on a shortest path between any other pair of nodes (Bastille-Rousseau et al., 2018). To convert simulated trajectories into a network, we followed Bastille-Rousseau et al. (2018) and overlaid the study area (including the buffer) with a raster containing 2.5 km x 2.5 km raster-cells, where the center of each raster-cell served as node in the final network. To identify edges (i.e. connections) between the nodes, we used the simulated trajectories and determined all transitions occurring from one cell to another, as well as the frequency at which those transitions occurred (see also Appendix A4). This resulted in an edge-list that we translated into a weighted network using the r-package `igraph` (Csardi and Nepusz, 2006). The final weight of each edge was determined by the frequency of transitions, yet because `igraph` handles edge weights ( $\omega$ ) as costs, we inverted the traversal-frequency through each raster-cell by applying  $\omega = \frac{\text{mean}(\text{TraversalFrequency})}{\text{TraversalFrequency}_i}$ . Consequently, regularly used edges received small weights (i.e. low costs) and vice versa. We used the weighted network to calculate betweenness scores for all network nodes.

#### 2.4.3 Inter-Patch Connectivity Map

To examine the presence and intensity of functional links (i.e. connections) between patches within the study area, we calculated inter-patch connectivity (e.g. Gustafson and Gardner, 1996, Kanagaraj et al., 2013). For this, we computed the relative frequency at which dispersers originating from one patch successfully moved into another patch. We considered

260 movements between patches as successful if an individual's dispersal trajectory originating  
261 from the source patch intersected with the target patch at least once. For each trajectory we  
262 also recorded the number of steps required to reach the first intersection with the respective  
263 patch, allowing us to compute the average dispersal durations from one patch to another.  
264 In summary, we determined *if* and *how often* dispersers moved between certain patches, as  
265 well as *how long* individuals had to move to make these connections. In our case study,  
266 we used NPs as patches to determine inter-patch connectivity, hence we'll use the terms  
267 interchangeably from here on. The decision to focus on NPs was purely out of simplicity  
268 and should not imply that dispersal between other areas is impossible.

#### 269 **2.4.4 Validation**

270 To validate our predictions of connectivity, we utilized additional dispersal data that was  
271 collected on eight dispersing coalitions between 2019 and 2022 (totalling to 2'668 GPS  
272 locations). We used path selection analysis (PSF, Cushman and Lewis, 2010) to assess  
273 if observed dispersal trajectories followed areas of high predicted connectivity. Similar to  
274 SSF, PSF enables to detect selection for certain features by comparing observed paths to  
275 randomly generated paths. Here, we paired each observed path with 50 random paths  
276 that we generated by randomly rotating and shifting observed paths by a random angle  
277  $\alpha \sim U(-\pi, +\pi)$  and a random distance  $d \sim U(0 \text{ km}, 50 \text{ km})$ . Along each path, we then  
278 extracted connectivity values from the heatmap (see above) generated after 68, 125, 250,  
279 500, and 2'000 simulated steps, respectively. Finally, we ran conditional logistic regression  
280 to contrast observed and random paths. In case of systematic selection for high-connectivity  
281 areas, the regression coefficients from the corresponding conditional logistic regression model  
282 should be positive.

## 283 **3 Results**

284 The most parsimonious movement model consisted of movement covariates, habitat covari-  
285 ates, as well as several of their interactions, thus suggesting that movement behavior during  
286 dispersal depended on habitat conditions (Figure 3a, Table S1 and Table S2). Although  
287 multiple models received an AIC weight  $> 0$  (Table S1), we only considered results from  
288 the most parsimonious model for simplicity. This decision only marginally influenced sub-  
289 sequent steps as all models with positive AIC weights retained similar covariates (Table  
290 S1). The k-fold cross-validation showed that the final model substantially outperformed a  
291 random guess and provided reliable predictions (i.e. confidence intervals of  $\bar{r}_{s,realized}$  and

*292*  $\bar{r}_{s,random}$  did not overlap). Moreover, the model correctly assigned high selection scores  
*293* to realized steps (Figure 3b), indicating a good fit between predictions and observations.  
*294* As can be taken from the Spearman rank correlation coefficient, the inclusion of several  
*295* interactions between movement and habitat covariates significantly improved model per-  
*296* formance ( $\bar{r}_{s,realized} = -0.65; 95\% - CI = [-0.67, -0.64]$ ), compared to the base model  
*297* ( $\bar{r}_{s,realized} = -0.55; 95\% - CI = [-0.57, -0.52]$ ; Hofmann et al., 2021a). Our validation  
*298* of the resulting connectivity maps using independent dispersal data showed that dispersers  
*299* preferentially followed areas of high predicted connectivity, as coefficients from the PSF  
*300* models were all significantly greater than zero (Figure 3c). The movement model thus  
*301* successfully predicted functional connectivity.

*302* Plots that aid with the interpretation of the most parsimonious movement model are pro-  
*303* vided in Figure S3 and suggest that, under average conditions, dispersing wild dogs avoided  
*304* moving through water, woodlands, and areas dominated by humans, but preferred moving  
*305* across shrublands or grasslands (Figure 3a). Dispersers realized shorter steps (indicating  
*306* slower movements) in areas covered by water or woodland, while realizing larger steps in  
*307* areas dominated by shrubs or grass (Figure 3a). We found a particularly large effect for the  
*308* variable **LowActivity**, suggesting that dispersing wild dogs moved substantially faster during  
*309* twilight and at night (i.e. between 17:00 and 09:00 o'clock; Figure 3a). Although dispersers  
*310* revealed a preference for directional movements (i.e. low turning angles), especially when  
*311* moving quickly, they did less so in proximity to humans or water, resulting in more tortuous  
*312* movements in such areas (Figure 3a).

### *313* 3.1 Dispersal Simulation

*314* Dispersal simulations based on the most parsimonious movement model proved useful for  
*315* assessing landscape connectivity. Of the 50,000 simulated dispersal trajectories that orig-  
*316* inated from the main study area, only 4.5% reached a map boundary, suggesting that we  
*317* successfully mitigated biases from boundary effects. Moreover, our examination of the rel-  
*318* ative traversal frequency across all checkpoints showed that the relative traversal frequency  
*319* reached a steady state after 10,500 simulated dispersal trajectories (Figure S4). Although  
*320* variability in the relative traversal frequency kept decreasing as we increased the number of  
*321* simulated dispersers, the marginal benefit of simulating additional trajectories diminished  
*322* quickly (Figure S4).

323 **3.2 Heatmap**

324 The heatmap (Figure 4), which resulted from the summation of all simulated dispersal tra-  
325 jectories, allowed us to pinpoint areas that were frequently visited and enabled us to compare  
326 areas inside and outside the KAZA-TFCA borders with respect to the intensity at which they  
327 were used for dispersal. For instance, we could deduct that areas inside the KAZA-TFCA  
328 were frequently traversed by dispersers (median traversal frequency inside KAZA-TFCA  
329 = 166, IQR = 274, Figure S7a), whereas areas beyond the KAZA-TFCA boundary were  
330 comparatively rarely visited (median traversal frequency outside KAZA-TFCA = 61, IQR  
331 = 133, Figure S7a). Most notably, the region in northern Botswana south of the Linyanti  
332 swamp appeared to serve as highly frequented dispersal hotspot (median traversal frequency  
333 = 987, IQR = 558). Aside from revealing movement hotspots, the heatmap also provided in-  
334 formation on areas that appeared to hinder movement. For example, extensive water bodies,  
335 such as the Okavango Delta, the Makgadikgadi Pan, and the Linyanti swamp, substantially  
336 restricted dispersal movements and limited realized connectivity inside the KAZA-TFCA.  
337 Similarly, the landscapes of Zambia and Zimbabwe were only rarely used for dispersal,  
338 even within the KAZA-TFCA boundaries (Figure S8a). Despite the fact that the heatmap  
339 improved our understanding of the frequency at which areas were traversed by simulated  
340 dispersers, it seemed impractical to pinpoint dispersal corridors.

341 **3.3 Betweenness**

342 The betweenness map (Figure 5) revealed several distinct dispersal corridors that run across  
343 the study area. In comparison to the heatmap, the betweenness map was less biased towards  
344 areas with many dispersers and pronounced narrower, more linear routes that were used by  
345 simulated individuals to move between regions. Again, northern Botswana emerged as a  
346 wild dog dispersal corridor that connected more remote regions in the study area. Towards  
347 east, the extension of this corridor ran through Chobe NP into Hwange NP. From there,  
348 a further extension connected to Matusadona NP in Zimbabwe. Northwest of the Linyanti  
349 ecosystem, a major corridor expanded into Angola, where it split and finally traversed over  
350 a long stretch of unprotected area into Zambia's Kafue NP. Several additional corridors  
351 with lower betweenness scores emerged, yet most of them ran within the KAZA-TFCA  
352 boundaries (median betweenness inside KAZA-TFCA =  $6.947 \times 10^6$ , IQR =  $54.311 \times 10^6$ ,  
353 Figure S7b). Consequently, only few corridors directly linked the peripheral regions of the  
354 KAZA-TFCA and passed through unprotected areas outside its borders (mean betweenness  
355 outside KAZA-TFCA =  $2.685 \times 10^6$ , IQR =  $9.891 \times 10^6$ , Figure S7b).

356 **3.4 Inter-Patch Connectivity**

357 The inter-patch connectivity map showed that the relative frequency at which simulated  
358 dispersal trajectories moved from one patch to another varied, as did the average dispersal  
359 duration between patches (Figure 6). The map thereby completed the picture on connectiv-  
360 ity and provided valuable insights into the frequency and duration of connections between  
361 patches. For some patches, we also detected imbalances between the number of incoming  
362 and outgoing links, hinting at possible source-sink dynamics. From Chobe NP, for instance,  
363 510 individuals reached the Moremi NP, yet the opposite route was only realized by 340  
364 individuals. Relative to the number of simulated individuals, however, these numbers corre-  
365 spond to fractions of 50% and 68%, respectively. Overall, inter-patch connectivity between  
366 patches in Angola, Namibia, Botswana, and Zimbabwe appeared to be high; between 54%  
367 and 87% of individuals originating from a patch in these countries successfully moved into  
368 at least one other patch (Figure S9a). Conversely, only 19% of the dispersers leaving from  
369 a patch in Zambia managed to find their way into some other patch (Figure S9b). Prior  
370 to reaching another patch, individuals from Angola, Namibia, Botswana, Zimbabwe, and  
371 Zambia had to move for an average of 630, 640, 940, 1045, and 890 steps, respectively. Fur-  
372 thermore, it appeared that the corridor previously identified on Figure 6 between Angola's  
373 NPs and the Kafue NP in Zambia is only rarely realized.

374 **4 Discussion**

375 Here, we presented a simple three-step approach to assess landscape connectivity via simu-  
376 lated dispersal trajectories and we demonstrated its application using empirical data from  
377 a free-ranging population of African wild dogs. In step one, we used ISSFs to parametrize a  
378 fully mechanistic movement model describing how individuals move through the landscape.  
379 Aside from rendering habitat preferences, the model also encapsulated movement prefer-  
380 ences and potential interactions between movement and habitat preferences. In step two,  
381 we employed the movement model and simulated dispersal trajectories across the landscape.  
382 In comparison to more traditional connectivity modeling techniques, such simulations re-  
383 quire fewer unrealistic assumptions about dispersal and enable the derivation of multiple  
384 connectivity metrics. Hence, in step three, we translated the simulated trajectories into  
385 three complementary connectivity maps, each emphasizing a different aspect of landscape  
386 connectivity (e.g. frequently traversed areas, critical dispersal corridors and bottlenecks,  
387 and the presence and intensity of functional links between suitable patches).

Results on the habitat kernel from our model showed that dispersers avoided areas dominated by humans and covered by water, but selected for regions with open grassland in the vicinity to water bodies. This largely complied with previous studies that investigated habitat selection by dispersing wild dogs (Davies-Mostert et al., 2012; Masenga et al., 2016; Woodroffe et al., 2019; O'Neill et al., 2020; Hofmann et al., 2021a). However, instead of merely generating insights on dispersers' habitat preferences, the ISSF framework also permitted us to model several additional complexities common to dispersal. For instance, by including the interactions  $\cos(\text{ta}):sl$  and  $\cos(\text{ta}):\log(sl)$ , we could accommodate that dispersers exhibit turning angles that are correlated with step lengths, meaning that turning angles tend to be smaller when individuals move fast. Although similar autocorrelations could be incorporated by sampling step lengths and turning angles from copula probability distributions (Hodel and Fieberg, 2022), the ISSF framework allowed us to conveniently model such peculiarities directly in the movement model. While we only considered first order autocorrelation, i.e. correlation between two consecutive steps, higher order autocorrelation is conceivable and may be desirable to model (Dray et al., 2010; McClintock et al., 2012). However, this will require vast amounts of GPS data that are not interrupted by missing fixes; something that is rarely achieved in reality (Graves and Waller, 2006). The power and flexibility of ISSFs to model additive effects between habitat and movement covariates (Avgar et al., 2016; Signer et al., 2017) furthermore allowed us to formally capture that dispersing wild dogs move slower and more tortuous in areas covered by water. Such effects may be of limited interest and novelty from a biological perspective, yet they are important to be considered when simulating dispersal, in particular if one is interested in estimating dispersal durations between habitat patches. Overall, the inclusion of interactions between habitat and movement covariates in our movement model lead to a significant improvement in predictive performance compared to an earlier model that omitted such interactions (Hofmann et al., 2021a).

Each of the three connectivity maps derived from simulated dispersal trajectories highlighted a different aspect of landscape connectivity. The heatmap was most suitable for pinpointing frequently traversed areas and showed that an exceptionally large number of dispersers moved through the regions of the Moremi NP and the Chobe NP in northern Botswana. Hofmann et al. (2021a) previously identified the same area as potential dispersal hotspot using LCPA, however, following their analysis it was not clear whether this was the consequence of the central location of the region and connections being enforced between predefined start and endpoints. Contrary to LCPA, a simulation-based approach as pre-

sented here does not require predefined endpoints, as endpoints emerge naturally from the simulated dispersal trajectories. This is especially useful for dispersal studies, where known endpoints are usually an unrealistic assumption (Elliot et al., 2014; Abrahms et al., 2017; Cozzi et al., 2020). The fact that the same region was emphasized using vastly different methods to model connectivity thus reinforces our notion that the area is of exceptional importance to dispersing wild dogs. Because simulated individuals are not forced to move towards certain endpoints, a simulation-based approach not only lends itself to study landscape connectivity, but also to uncover potential dispersal traps (Van der Meer et al., 2014) or areas with a high susceptibility for human wildlife conflicts (Cushman et al., 2018). Using independent dispersal data we showed that dispersers indeed followed areas of high predicted connectivity. Importantly, however, these predictions were based on a scenario of a relatively extended flood, which may not have accurately represented environmental conditions for dispersers moving through areas affected by the flood. Accounting for such differences would have improved the predictive performance of our model.

In contrast to the heatmap, the betweenness map emphasized relatively narrow and linear movement routes. It thus facilitated the identification of discrete movement corridors. While in some cases both the heatmap and the betweenness map attributed a high importance to the same areas (e.g. northern Botswana), little consensus was found for other regions. For instance, the stretch of unprotected land between Luengue-Luiana NP in Angola and the Kafue NP in Zambia was characterized by a high betweenness-scores, yet it only received low scores on the heatmap. This is due to the differential way in which the maps view connectivity. While the heatmap attributes a high connectivity to areas that are frequently traversed, it does not distinguish between areas that truly bring individuals into other regions of the study area and regions that lead into ecological traps. The converse is true on the betweenness map, as it strictly highlights regions that promote movement into other areas of the landscape and thus promote gene-flow. However, neither of the two maps provides insights into functional links between distinct habitat patches or how connections depend on the dispersal duration. For this reason, we also produced a map of inter-patch connectivity. This map depicted the frequency at which simulated individuals moved between patches as well as the average dispersal duration (in steps) required to realize them. Calculating dispersal durations was only possible because trajectories were simulated spatially and temporally explicitly, something that is currently unfeasible with LCPA or CT. An explicit representation of time enables answerings questions such as: “*How long will it take a disperser to move from A to B?*” or “*Is it possible for a disperser to move from A to B within*

456 *X days?*”. Moreover, it yields opportunities to incorporate seasonality and to investigate  
457 whether dispersal corridors exist seasonally or all-year round (*dynamic connectivity*; Zeller  
458 et al., 2020). With LCPA or CT, seasonality can currently only be incorporated through  
459 the preparation of multiple permeability surfaces on which the same connectivity model is  
460 repeatedly applied (e.g. Osipova et al., 2019). With simulations from ISSFs, in contrast, the  
461 environment could change “as the dispersers move”, so that simulated trajectories would  
462 dynamically respond to seasonal fluctuations in the environment.

463 Our approach enabled us to translate a simple set of small-scale behavioral rules into  
464 large scale patterns of connectivity, something previously deemed computationally unfea-  
465 sible, yet critical for linking structural and functional connectivity (Doerr et al., 2011).  
466 Structural connectivity focuses purely on the spatial arrangement of suitable habitat in the  
467 landscape, whereas functional connectivity also takes into account a species dispersal ability  
468 and behavioral response to the landscape (Tischendorf and Fahrig, 2000). Functional con-  
469 nectivity is of greater interest to conservation scientists, yet is difficult to quantify (Baguette  
470 et al., 2013), which is why structural connectivity often serves as surrogate (Doerr et al.,  
471 2011; Fattebert et al., 2015). LCPA and CT incorporate functional aspects of connectivity  
472 through the permeability surface, which reflects a species habitat preferences and thus ren-  
473 ders behavioral impacts of the landscape on the focal species. Aside from rendering habitat  
474 preferences, our model also integrates peculiarities of the focal species movement behavior,  
475 thus adding further insights on functional connectivity. In addition, we successfully used in-  
476 dependent dispersal data to prove that our predictions of connectiviy aligned with observed  
477 functional connectivity patterns.

478 Despite the many benefits and great flexibility offered by simulations from ISSFs, one  
479 must also be aware of the associated limitations. For example, while our approach of simulat-  
480 ing dispersal proved useful to assess landscape connectivity, it was computationally costly.  
481 Simulating 80,000 dispersal trajectories for 2'000 steps across the KAZA-TFCA required  
482 five days of computation on a regular desktop machine (AMD Ryzen 7 2700X octa-core  
483 processor with 3.6 GHz, 64 GB of RAM). The long simulation time was primarily caused  
484 by the massive extent of the study area considered (ca. 1.3 Mio km<sup>2</sup>), the large number of  
485 simulated trajectories, and the fact that we extracted covariates along each step, rather than  
486 just at their start or endpoints. Most connectivity studies focus on smaller study areas (e.g.  
487 Kanagaraj et al., 2013; Clark et al., 2015; McClure et al., 2016; Abrahms et al., 2017; Zeller  
488 et al., 2020) and will therefore require fewer simulations and achieve faster simulation times  
489 (given the same spatial resolution). We also believe that fewer simulated trajectories will

often suffice, as the relative traversal frequency by simulated trajectories through randomly placed checkpoints across our study area converged already after 10,500 runs. The exact number of required simulations to achieve reliable estimates of connectivity will, of course, vary depending on the structure of the landscape and the dispersal capabilities of the focal species (Gustafson and Gardner, 1996). For species that disperse short distances through homogeneous environments, few simulations may suffice to gauge connectivity, whereas for species that disperse over long distances through heterogeneous habitats, a large number of simulations will be required to sufficiently explore the spectrum of possible routes. Finally, it may often suffice to extract covariates at each step's start or endpoints, thus considerably speeding up simulation times (Signer et al., 2017).

Aside from the computational requirements, simulations further entail several non-trivial but important modeling decisions. On four such decisions we would like to further elaborate: (1) the number of simulated individuals, (2) the location of source points, (3) the simulated dispersal duration, and (4) the behavior at map boundaries.

(1) When simulating dispersal trajectories, the modeler needs to decide on the number of simulated individuals. A higher number is always desirable, as each additional trajectory provides information about landscape connectivity. However, each additional simulation imposes computational costs, so a trade-off needs to be managed. Signer et al. (2017) proposed to handle the trade-off by simulating additional individuals only until the metrics of interest converge towards a steady state. Here, we used the relative traversal frequency as target metric and found that it converged already after 10'500 simulated individuals. The exact number of required individuals might, however, vary depending on the employed target metric and the anticipated connectivity map. More sophisticated target metrics than the relative traversal frequency, preferably tailored to different connectivity maps, need to be developed in the future.

(2) To initiate dispersers, a modeler needs to provide a set of source points at which the virtual dispersers are released. We placed source points within protected areas large enough to sustain viable wild dog populations, implicitly assuming that wild dogs primarily survive in large, formally protected areas (Davies-Mostert et al., 2012; Woodroffe and Sillero-Zubiri, 2012; Van der Meer et al., 2014). Moreover, we lacked precise knowledge about the distribution and abundance of wild dogs across protected areas, so we placed source points randomly within them. In cases where more detailed data about the distribution and abundance of the focal species are available, source points could be distributed accordingly. Alternatively, source points could be distributed homogeneously but later be weighted when

524 computing connectivity metrics. In any case, the challenge of selecting meaningful source  
525 points is not unique to individual-based simulations but also applies to LCPA and CT.

526 (3) The use of ISSFs to simulate dispersers requires deciding on the number of simulated  
527 steps (i.e. the simulated dispersal durations). If sufficient dispersal data of the focal species  
528 has been collected, dispersal durations could be sampled from observed dispersal events or  
529 from parametric distributions fit to observed data. Due to the low number of observed  
530 dispersal events, we opted against this solution and instead simulated all individuals for  
531 2,000 steps, which was at the upper end of observed dispersal durations in African wild  
532 dogs (Davies-Mostert et al., 2012; Masenga et al., 2016; Cozzi et al., 2020; Hofmann et al.,  
533 2021a). This approach had the advantage that it allowed us to systematically shorten the  
534 simulated trajectories after their simulation and thereby to investigate the sensitivity of our  
535 results with respect to exact dispersal durations (Figures S5 and S6).

536 (4) Unless simulated dispersal trajectories are strongly drawn towards a point of attraction  
537 inside the study area(e.g. Signer et al., 2017), some trajectories will inevitably approach  
538 one of the map boundaries. In this case, one or more of the generated random steps might  
539 leave the study area, making it impossible to compute a selection score. A possible solution  
540 is to simply terminate the simulation of the affected trajectory, assuming that the simulated  
541 individual has left the study area. However, this approach might produce ambiguous results  
542 in cases where many individuals are released near map borders, especially because already a  
543 single random step leaving the study area will break the simulation, thus resulting in biased  
544 connectivity estimates along map borders. Rather than breaking the simulation, we created  
545 a buffer zone (Koen et al., 2010) and resampled random steps until they fully lied within  
546 the study area. This proved to be an effective solution to overcome problems with boundary  
547 effects.

548 In summary, we proposed and applied a simple three-step approach that relies on ISSF-  
549 analysis and enables the simulation of dispersal trajectories and the assessment of landscape  
550 connectivity. The proposed approach overcomes several of the conceptual shortcomings  
551 inherent to LCPA and CT, such as the assumption of known endpoints, and provides a highly  
552 flexible tool for investigating connectivity. Moreover, the simulation of dispersal opens up  
553 new avenues for incorporating interactions between habitat and movement covariates and  
554 provides the foundation for a rich suite of complementary connectivity measures. With  
555 this work, we hope to have sparked interest in the application, optimization, or creation  
556 of methods to investigate dispersal and connectivity via individual-based simulations, while  
557 at the same time stressing some of the non-trivial modeling decisions involved. We also

558 hope to provide a useful framework that helps unifying and streamlining the application of  
559 individual-based simulations for assessing landscape connectivity.

## 560 **5 Authors' Contributions**

561 D.D.H., D.M.B., A.O. and G.C. conceived the study and designed methodology; D.M.B.,  
562 G.C., and J.W.M. collected the data; D.D.H. and D.M.B. analysed the data; G.C. and A.O.  
563 assisted with modeling; D.D.H., D.M.B., and G.C. wrote the first draft of the manuscript and  
564 all authors contributed to the drafts at several stages and gave final approval for publication.

## 565 **6 Data Availability**

566 GPS movement data of dispersing wild dogs is available on dryad (Hofmann et al., 2021b).  
567 Access to R-scripts that exemplify the application of the proposed approach using simulated  
568 data are provided through Github (<https://github.com/DavidDHofmann/DispersalSimulation>).  
569 In addition, all codes required to reproduce the African wild dog case study will be made  
570 available through an online repository at the time of publication.

## 571 **7 Acknowledgements**

572 We thank the Ministry of Environment and Tourism of Botswana for granting permission  
573 to conduct this research. We thank C. Botes, I. Clavadetscher, and G. Camenisch for  
574 assisting with wild dog immobilizations. We also thank B. Abrahms for sharing her data  
575 of three dispersing wild dogs. Furthermore, we would like to thank Johannes Signer for  
576 assisting with the simulation algorithm. This study was funded by Albert-Heim Foundation,  
577 Basler Stiftung für Biologische Forschung, Claraz Foundation, Idea Wild, Jacot Foundation,  
578 National Geographic Society, Parrotia Stiftung, Stiftung Temperatio, Wilderness Wildlife  
579 Trust, Forschungskredit of the University of Zürich (grant no. FK-21-091), and a Swiss  
580 National Science Foundation grant (no. 31003A\_182286) to A. Ozgul.

## 581 **8 Conflict of Interest**

582 All authors declare that they have no conflicts of interest.

## 583 References

- 584 Abrahms, B., Sawyer, S. C., Jordan, N. R., McNutt, J. W., Wilson, A. M., and Brashares,  
585 J. S. (2017). Does Wildlife Resource Selection Accurately Inform Corridor Conservation?  
586 *Journal of Applied Ecology*, 54(2):412–422.
- 587 Adriaensen, F., Chardon, J., De Blust, G., Swinnen, E., Villalba, S., Gulinck, H., and  
588 Matthysen, E. (2003). The Application of Least-Cost Modelling as a Functional Landscape  
589 Model. *Landscape and Urban Planning*, 64(4):233–247.
- 590 Allen, C. H., Parrott, L., and Kyle, C. (2016). An Individual-Based Modelling Approach to  
591 Estimate Landscape Connectivity for Bighorn Sheep (*Ovis canadensis*). *PeerJ*, 4:e2001.
- 592 Avgar, T., Lele, S. R., Keim, J. L., and Boyce, M. S. (2017). Relative Selection Strength:  
593 Quantifying Effect Size in Habitat- and Step-Selection Inference. *Ecology and Evolution*,  
594 7(14):5322–5330.
- 595 Avgar, T., Potts, J. R., Lewis, M. A., and Boyce, M. S. (2016). Integrated Step Selection  
596 Analysis: Bridging the Gap Between Resource Selection and Animal Movement. *Methods  
597 in Ecology and Evolution*, 7(5):619–630.
- 598 Baguette, M., Blanchet, S., Legrand, D., Stevens, V. M., and Turlure, C. (2013). Indi-  
599 vidual Dispersal, Landscape Connectivity and Ecological Networks. *Biological Reviews*,  
600 88(2):310–326.
- 601 Bastille-Rousseau, G., Douglas-Hamilton, I., Blake, S., Northrup, J. M., and Wittemyer,  
602 G. (2018). Applying Network Theory to Animal Movements to Identify Properties of  
603 Landscape Space Use. *Ecological Applications*, 28(3):854–864.
- 604 Behr, D. M., McNutt, J. W., Ozgul, A., and Cozzi, G. (2020). When to Stay and When  
605 to Leave? Proximate Causes of Dispersal in an Endangered Social Carnivore. *Journal of  
606 Animal Ecology*, 89(10):2356–2366.
- 607 Brennan, A., Beytell, P., Aschenborn, O., Du Preez, P., Funston, P., Hanssen, L., Kilian,  
608 J., Stuart-Hill, G., Taylor, R., and Naidoo, R. (2020). Characterizing Multispecies  
609 Connectivity Across a Transfrontier Conservation Landscape. *Journal of Applied Ecology*,  
610 57:1700–1710.
- 611 Brooks, M. E., Kristensen, K., van Benthem, K. J., Magnusson, A., Berg, C. W., Nielsen,  
612 A., Skaug, H. J., Maechler, M., and Bolker, B. M. (2017). glmmTMB Balances Speed and  
613 Flexibility among Packages for Zero-Inflated Generalized Linear Mixed Modeling. *The R  
614 Journal*, 9(2):378–400.
- 615 Brown, J. H. and Kodric-Brown, A. (1977). Turnover Rates in Insular Biogeography: Effect  
616 of Immigration on Extinction. *Ecology*, 58(2):445–449.
- 617 Burnham, K. P. and Anderson, D. R. (2002). *Model Selection and Multimodel Inference: A  
618 Practical Information-Theoretic Approach*. Springer Science & Business Media, Ney York,  
619 NY, USA.
- 620 Clark, J. D., Laufenberg, J. S., Davidson, M., and Murrow, J. L. (2015). Connectivity among  
621 Subpopulations of Louisiana Black Bears as Estimated by a Step Selection Function. *The  
622 Journal of Wildlife Management*, 79(8):1347–1360.
- 623 Clobert, J., Baguette, M., Benton, T. G., and Bullock, J. M. (2012). *Dispersal Ecology and  
624 Evolution*. Oxford University Press, Oxford, UK.
- 625 Cozzi, G., Behr, D. M., Webster, H. S., Claase, M., Bryce, C. M., Modise, B., Mcnutt, J. W.,  
626 and Ozgul, A. (2020). African Wild Dog Dispersal and Implications for Management. *The  
627 Journal of Wildlife Management*, pages 614–621.
- 628 Cozzi, G., Broekhuis, F., McNutt, J. W., Turnbull, L. A., Macdonald, D. W., and Schmid,  
629 B. (2012). Fear of the Dark or Dinner by Moonlight? Reduced Temporal Partitioning  
630 among Africa's Large Carnivores. *Ecology*, 93(12):2590–2599.

- 631 Creel, S., Merkle, J., Mweetwa, T., Becker, M. S., Mwape, H., Simpamba, T., and  
632 Simukonda, C. (2020). Hidden Markov Models Reveal a clear Human Footprint on the  
633 Movements of Highly Mobile African Wild Dogs. *Scientific reports*, 10(1):1–11.
- 634 Csardi, G. and Nepusz, T. (2006). The igraph Software Package for Complex Network  
635 Research. *InterJournal, Complex Systems*:1695.
- 636 Cushman, S. A., Elliot, N. B., Bauer, D., Kesch, K., Bahaa-el din, L., Bothwell, H., Flyman,  
637 M., Mtare, G., Macdonald, D. W., and Loveridge, A. J. (2018). Prioritizing Core Areas,  
638 Corridors and Conflict Hotspots for Lion Conservation in Southern Africa. *PLOS ONE*,  
639 13(7):e0196213.
- 640 Cushman, S. A. and Lewis, J. S. (2010). Movement Behavior Explains Genetic Differentiation  
641 in American Black Bears. *Landscape Ecology*, 25(10):1613–1625.
- 642 Davies-Mostert, H. T., Kamler, J. F., Mills, M. G. L., Jackson, C. R., Rasmussen, G. S. A.,  
643 Groom, R. J., and Macdonald, D. W. (2012). Long-Distance Transboundary Dispersal  
644 of African Wild Dogs among Protected Areas in Southern Africa. *African Journal of  
645 Ecology*, 50(4):500–506.
- 646 Diniz, M. F., Cushman, S. A., Machado, R. B., and De Marco Júnior, P. (2019). Landscape  
647 Connectivity Modeling from the Perspective of Animal Dispersal. *Landscape Ecology*,  
648 35:41–58.
- 649 Doerr, V. A. J., Barrett, T., and Doerr, E. D. (2011). Connectivity, Dispersal Behaviour  
650 and Conservation under Climate Change: A Response to Hodgson et al.: Connectivity  
651 and Dispersal Behaviour. *Journal of Applied Ecology*, 48(1):143–147.
- 652 Dray, S., Royer-Carenzi, M., and Calenge, C. (2010). The Exploratory Analysis of Autocor-  
653 relation in Animal-Movement Studies. *Ecological Research*, 25(3):673–681.
- 654 Eddelbuettel, D. (2013). *Seamless R and C++ Integration with Rcpp*. Springer, New York.  
655 ISBN 978-1-4614-6867-7.
- 656 Eddelbuettel, D. and Balamuta, J. J. (2018). Extending extitR with extitC++: A Brief  
657 Introduction to extitRcpp. *The American Statistician*, 72(1):28–36.
- 658 Eddelbuettel, D. and François, R. (2011). Rcpp: Seamless R and C++ Integration. *Journal  
659 of Statistical Software*, 40(8):1–18.
- 660 Elliot, N. B., Cushman, S. A., Macdonald, D. W., and Loveridge, A. J. (2014). The Devil  
661 is in the Dispersers: Predictions of Landscape Connectivity Change with Demography.  
662 *Journal of Applied Ecology*, 51(5):1169–1178.
- 663 Fahrig, L. (2003). Effects of Habitat Fragmentation on Biodiversity. *Annual Review of  
664 Ecology, Evolution, and Systematics*, 34(1):487–515.
- 665 Fattebert, J., Robinson, H. S., Balme, G., Slotow, R., and Hunter, L. (2015). Structural  
666 Habitat Predicts Functional Dispersal Habitat of a Large Carnivore: How Leopards  
667 Change Spots. *Ecological Applications*, 25(7):1911–1921.
- 668 Fieberg, J., Signer, J., Smith, B., and Avgar, T. (2021). A ‘How to’ Guide for Interpreting  
669 Parameters in Habitat-Selection Analyses. *Journal of Animal Ecology*, 90(5):1027–1043.
- 670 Fortin, D., Beyer, H. L., Boyce, M. S., Smith, D. W., Duchesne, T., and Mao, J. S. (2005).  
671 Wolves Influence Elk Movements: Behavior Shapes a Trophic Cascade in Yellowstone  
672 National Park. *Ecology*, 86(5):1320–1330.
- 673 Fortin, D., Fortin, M.-E., Beyer, H. L., Duchesne, T., Courant, S., and Dancose, K. (2009).  
674 Group-Size-Mediated Habitat Selection and Group Fusion–Fission Dynamics of Bison  
675 under Predation Risk. *Ecology*, 90(9):2480–2490.
- 676 Frankham, R., Briscoe, D. A., and Ballou, J. D. (2002). *Introduction to Conservation  
677 Genetics*. Cambridge University Press, Cambridge, UK.

- 678 Graves, T. A. and Waller, J. S. (2006). Understanding the Causes of Missed Global Positioning System Telemetry Fixes. *Journal of Wildlife Management*, 70(3):844–851.
- 680 Gustafson, E. J. and Gardner, R. H. (1996). The Effect of Landscape Heterogeneity on the Probability of Patch Colonization. *Ecology*, 77(1):94–107.
- 682 Hanski, I. (1999). *Metapopulation Ecology*. Oxford University Press.
- 683 Hauenstein, S., Fattebert, J., Grüebler, M. U., Naef-Daenzer, B., Pe'er, G., and Hartig, F. (2019). Calibrating an Individual-Based Movement Model to Predict Functional Connectivity for Little Owls. *Ecological Applications*, 29(4):e01873.
- 686 Hijmans, R. J. (2021). *terra: Spatial Data Analysis*. R package version 1.2-10.
- 687 Hodel, F. H. and Fieberg, J. R. (2022). Circular-Linear Copulae for Animal Movement Data. *Methods in Ecology and Evolution*, pages 2041–210X.13821.
- 689 Hofmann, D. D., Behr, D. M., McNutt, J. W., Ozgul, A., and Cozzi, G. (2021a). Bound within boundaries: Do protected areas cover movement corridors of their most mobile, protected species? *Journal of Applied Ecology*, 58(6):1133–1144. Publisher: Wiley Online Library.
- 693 Hofmann, D. D., Behr, D. M., McNutt, J. W., Ozgul, A., and Cozzi, G. (2021b). Data from: Bound within Boundaries: Do Protected Areas Cover Movement Corridors of their Most Mobile, Protected Species? Dryad Digital Repository. <https://doi:10.5061/dryad.dncjsxkzn>.
- 697 Kanagaraj, R., Wiegand, T., Kramer-Schadt, S., and Goyal, S. P. (2013). Using Individual-Based Movement Models to Assess Inter-Patch Connectivity for Large Carnivores in Fragmented Landscapes. *Biological Conservation*, 167:298 – 309.
- 700 Koen, E. L., Bowman, J., Sadowski, C., and Walpole, A. A. (2014). Landscape Connectivity for Wildlife: Development and Validation of Multispecies Linkage Maps. *Methods in Ecology and Evolution*, 5(7):626–633.
- 703 Koen, E. L., Garroway, C. J., Wilson, P. J., and Bowman, J. (2010). The Effect of Map Boundary on Estimates of Landscape Resistance to Animal Movement. *PLoS ONE*, 5(7):e11785.
- 706 Landguth, E. L., Hand, B. K., Glassy, J., Cushman, S. A., and Sawaya, M. A. (2012). UNICOR: A Species Connectivity and Corridor Network Simulator. *Ecography*, 35(1):9–14.
- 709 LaPoint, S., Gallery, P., Wikelski, M., and Kays, R. (2013). Animal Behavior, Cost-Based Corridor Models, and Real Corridors. *Landscape Ecology*, 28(8):1615–1630.
- 711 Latham, A. D. M., Latham, M. C., Boyce, M. S., and Boutin, S. (2011). Movement Responses by Wolves to Industrial Linear Features and Their Effect on Woodland Caribou in Northeastern Alberta. *Ecological Applications*, 21(8):2854–2865.
- 714 Leigh, K. A., Zenger, K. R., Tammen, I., and Raadsma, H. W. (2012). Loss of Genetic Diversity in an Outbreeding Species: Small Population Effects in the African Wild Dog (*Lycaon pictus*). *Conservation Genetics*, 13(3):767–777.
- 717 MacArthur, R. H. and Wilson, E. O. (2001). *The Theory of Island Biogeography*, volume 1. Princeton University Press, Princeton, New Jersey, USA.
- 719 Martensen, A. C., Saura, S., and Fortin, M. (2017). Spatio-Temporal Connectivity: Assessing the Amount of Reachable Habitat in Dynamic Landscapes. *Methods in Ecology and Evolution*, 8(10):1253–1264.
- 722 Masenga, E. H., Jackson, C. R., Mjingo, E. E., Jacobson, A., Riggio, J., Lyamuya, R. D., Fyumagwa, R. D., Borner, M., and Røskift, E. (2016). Insights into Long-Distance Dispersal by African Wild Dogs in East Africa. *African Journal of Ecology*, 54(1):95–98.

- 725 McClintock, B. T., King, R., Thomas, L., Matthiopoulos, J., McConnell, B. J., and Morales,  
726 J. M. (2012). A General Discrete-Time Modeling Framework for Animal Movement Using  
727 Multistate Random Walks. *Ecological Monographs*, 82(3):335–349.
- 728 McClure, M. L., Hansen, A. J., and Inman, R. M. (2016). Connecting Models to Movements:  
729 Testing Connectivity Model Predictions against Empirical Migration and Dispersal Data.  
730 *Landscape Ecology*, 31(7):1419–1432.
- 731 McNutt, J. (1996). Sex-Biased Dispersal in African Wild Dogs (*Lycaon pictus*). *Animal  
732 Behaviour*, 52(6):1067–1077.
- 733 McRae, B. H. (2006). Isolation by Resistance. *Evolution*, 60(8):1551–1561.
- 734 McRae, B. H., Dickson, B. G., Keitt, T. H., and Shah, V. B. (2008). Using Circuit Theory to  
735 Model Connectivity in Ecology, Evolution, and Conservation. *Ecology*, 89(10):2712–2724.
- 736 Muff, S., Signer, J., and Fieberg, J. (2020). Accounting for Individual-Specific Variation in  
737 Habitat-Selection Studies: Efficient Estimation of Mixed-Effects Models Using Bayesian  
738 or Frequentist Computation. *Journal of Animal Ecology*, 89(1):80–92.
- 739 Osipova, L., Okello, M. M., Njumbi, S. J., Ngene, S., Western, D., Hayward, M. W., and  
740 Balkenhol, N. (2019). Using Step-Selection Functions to Model landscape Connectivity  
741 for African Elephants: Accounting for Variability across Individuals and Seasons. *Animal  
742 Conservation*, 22(1):35–48.
- 743 O'Neill, H. M. K., Durant, S. M., and Woodroffe, R. (2020). What Wild Dogs Want: Habitat  
744 Selection Differs across Life Stages and Orders of Selection in a Wide-Ranging Carnivore.  
745 *BMC Zoology*, 5(1).
- 746 Panzacchi, M., Van Moorter, B., Strand, O., Saerens, M., Kivimäki, I., St. Clair, C. C.,  
747 Herfindal, I., and Boitani, L. (2016). Predicting the Continuum Between Corridors and  
748 Barriers to Animal Movements Using Step Selection Functions and Randomized Shortest  
749 Paths. *Journal of Animal Ecology*, 85(1):32–42.
- 750 Perrin, N. and Mazalov, V. (2000). Local Competition, Inbreeding, and the Evolution of  
751 Sex-Biased Dispersal. *The American Naturalist*, 155(1):116–127.
- 752 Pinto, N. and Keitt, T. H. (2009). Beyond the Least-Cost Path: Evaluating Corridor  
753 Redundancy Using a Graph-Theoretic Approach. *Landscape Ecology*, 24(2):253–266.
- 754 Pomilia, M. A., McNutt, J. W., and Jordan, N. R. (2015). Ecological Predictors of African  
755 Wild Dog Ranging Patterns in Northern Botswana. *Journal of Mammalogy*, 96(6):1214–  
756 1223.
- 757 Potts, J. R., Bastille-Rousseau, G., Murray, D. L., Schaefer, J. A., and Lewis, M. A. (2013).  
758 Predicting local and non-local effects of resources on animal space use using a mechanistic  
759 step selection model. *Methods in Ecology and Evolution*, 5(3):253–262.
- 760 R Core Team (2022). *R: A Language and Environment for Statistical Computing*. R Foun-  
761 dation for Statistical Computing, Vienna, Austria.
- 762 Rudnick, D., Ryan, S., Beier, P., Cushman, S., Dieffenbach, F., Epps, C., Gerber, L., Hart-  
763 ter, J., Jenness, J., Kintsch, J., Merenlender, A., Perkl, R., Perziosi, D., and Trombulack,  
764 S. (2012). The Role of Landscape Connectivity in Planning and Implementing Conserva-  
765 tion and Restoration Priorities. *Issues in Ecology*.
- 766 Sawyer, S. C., Epps, C. W., and Brashares, J. S. (2011). Placing Linkages among Fragmented  
767 Habitats: Do Least-Cost Models Reflect How Animals Use Landscapes? *Journal of  
768 Applied Ecology*, 48(3):668–678.
- 769 Signer, J., Fieberg, J., and Avgar, T. (2017). Estimating Utilization Distributions from  
770 Fitted Step-Selection Functions. *Ecosphere*, 8(4):e01771.

- 771 Tischendorf, L. and Fahrig, L. (2000). On the Usage and Measurement of Landscape Con-  
772 nectivity. *Oikos*, 90(1):7–19.
- 773 Turchin, P. (1998). *Quantitative Analysis of Movement: Measuring and Modeling Population*  
774 *Redistribution in Plants and Animals*. Sinauer Associates, Sunderland, MA, USA.
- 775 Van der Meer, E., Fritz, H., Blinston, P., and Rasmussen, G. S. (2014). Ecological Trap in  
776 the Buffer Zone of a Protected Area: Effects of Indirect Anthropogenic Mortality on the  
777 African Wild Dog (*Lycaon pictus*). *Oryx*, 48(2):285–293.
- 778 Vasudev, D., Fletcher, R. J., Goswami, V. R., and Krishnadas, M. (2015). From Disper-  
779 sal Constraints to Landscape Connectivity: Lessons from Species Distribution Modeling.  
780 *Ecography*, 38(10):967–978.
- 781 Whittingham, M. J., Stephens, P. A., Bradbury, R. B., and Freckleton, R. P. (2006). Why Do  
782 We Still Use Stepwise Modelling in Ecology and Behaviour? *Journal of Animal Ecology*,  
783 75(5):1182–1189.
- 784 Wolski, P., Murray-Hudson, M., Thito, K., and Cassidy, L. (2017). Keeping it Simple:  
785 Monitoring Flood Extent in Large Data-Poor Wetlands Using MODIS SWIR Data. *In-*  
786 *ternational Journal of Applied Earth Observation and Geoinformation*, 57:224–234.
- 787 Woodroffe, R., Rabaiotti, D., Ngatia, D. K., Smallwood, T. R. C., Strelbel, S., and O'Neill,  
788 H. M. K. (2019). Dispersal Behaviour of African Wild Dogs in Kenya. *African Journal*  
789 *of Ecology*.
- 790 Woodroffe, R. and Sillero-Zubiri, C. (2012). *Lycaon pictus*. *The IUCN Red List of Threatened*  
791 *Species*, 2012:e. T12436A1671116.
- 792 Zeller, K. A., Wattles, D. W., Bauder, J. M., and DeStefano, S. (2020). Forecasting Seasonal  
793 Habitat Connectivity in a Developing Landscape. *Land*, 9(7):233.

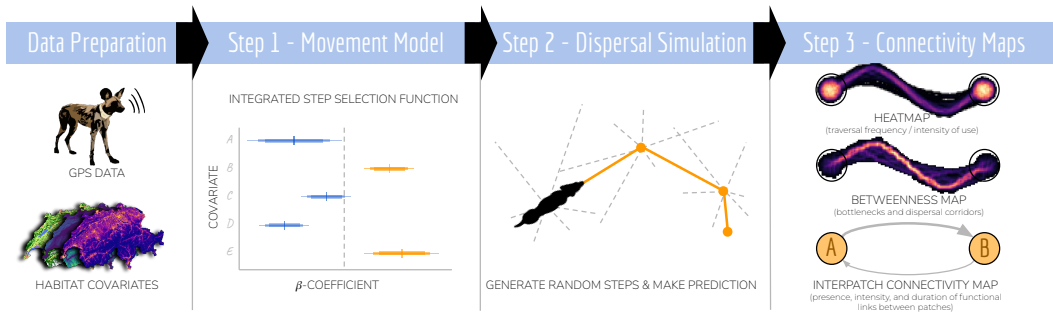


**Figure 1:** Flowchart of the simulation-based connectivity analysis. First, GPS data and habitat covariates must be collected. The combined data is then analyzed using an integrated step selection model (step 1). The parametrized model is then treated as an individual-based movement model and used to simulate dispersal trajectories (step 2). Ultimately, simulated trajectories are translated into a set of maps that are pertinent to landscape connectivity (step 3). This includes a heatmap, indicating the traversal frequency across each spatial unit of the study area, a betweenness map, highlighting movement corridors and bottlenecks, and, finally, an inter-patch connectivity map, where the frequency of connections and their average duration can be depicted.

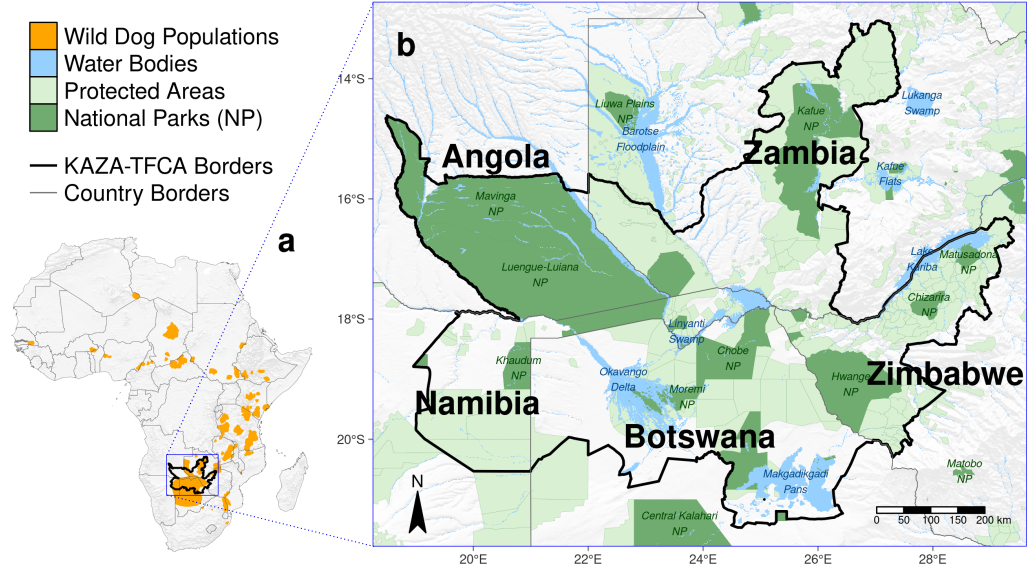


**Figure 2:** Illustration of the study area in southern Africa. (a) The study area was confined by a bounding box spanning the entire KAZA-TFCA which comprises parts of Angola, Namibia, Botswana, Zimbabwe, and Zambia. Data on remaining wild dog populations (orange) has been sourced from Woodroffe and Sillero-Zubiri (2012). (b) The KAZA-TFCA represents the world's largest terrestrial transfrontier conservation area and covers a total area of 520'000 km<sup>2</sup>. Its main purpose is to re-establish connectivity between already-existing NPs (dark green) and other protected areas (light green).

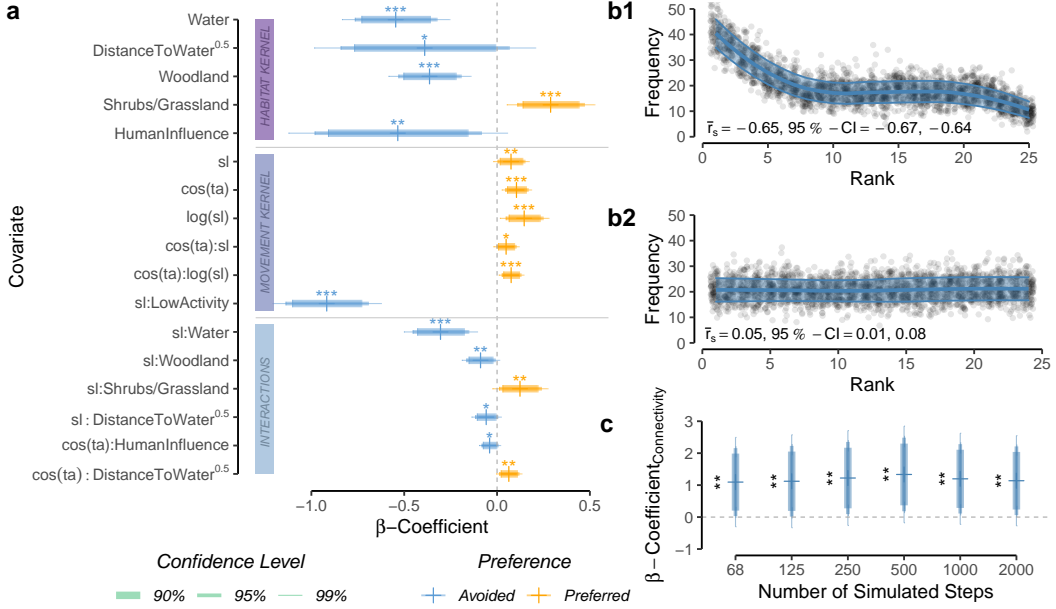


**Figure 3:** (a) Most parsimonious movement model for dispersing wild dogs. The model comprises a habitat kernel, a movement kernel, as well as their interactions. The horizontal line segments delineate the 90%, 95%, and 99% confidence-intervals for the respective  $\beta$ -coefficients. Significance codes: \*  $p < 0.10$ , \*\*  $p < 0.05$ , \*\*\*  $p < 0.01$ . (b) Results from the k-fold cross validation procedure. Subfigure b1 shows rank frequencies of realized steps according to model predictions with known preferences, whereas subfigure b2 shows rank frequencies of realized steps when assuming random preferences. The blue ribbon shows the prediction interval around a loess smoothing regression that we fitted to ease the interpretation of the plots. The significant correlation between rank and associated frequency in (b1) highlights that the most parsimonious model successfully outperformed a random guess (b2) and frequently assigned low ranks (i.e. high selection scores) to realized steps but only rarely high ranks (i.e. low selection scores). (c) Results from the PSF analysis using independent dispersal data show that dispersers preferably moved through areas where our heatmaps predicted high connectivity. Results are shown for heatmaps realized after 68, 125, 250, 500, and 2'000 simulated steps, respectively.

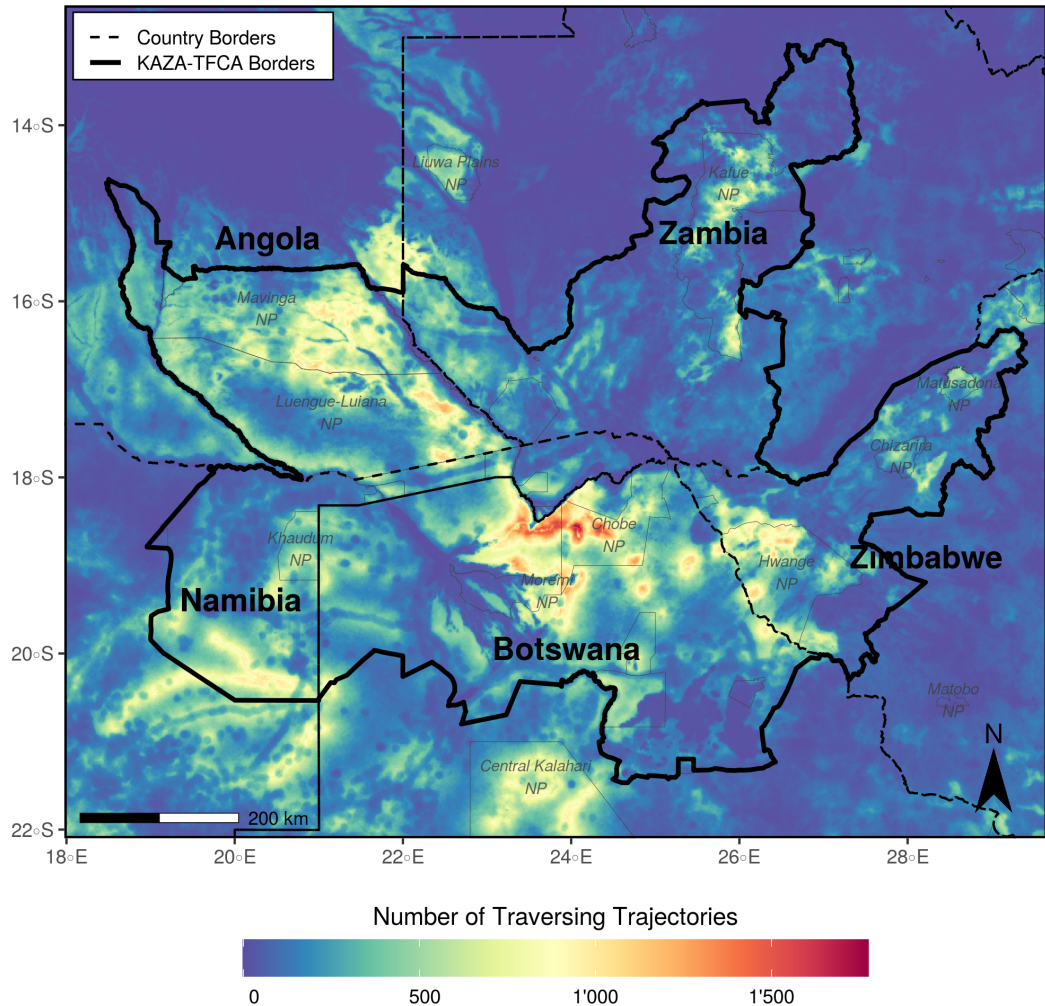


**Figure 4:** Heatmap showing traversal frequencies of 80'000 simulated dispersers moving 2'000 steps across the KAZA-TFCA. Simulations were based on an integrated step-selection model that we fitted to the movement data of dispersing African wild dogs. To generate the heatmap, we rasterized and tallied all simulated trajectories. Consequently, the map highlights areas that are frequently traversed. For spatial reference we plotted a few selected NPs (dark gray). Additional heatmaps showing the traversal frequency when individuals move fewer than 2'000 steps are provided in Figure S5.

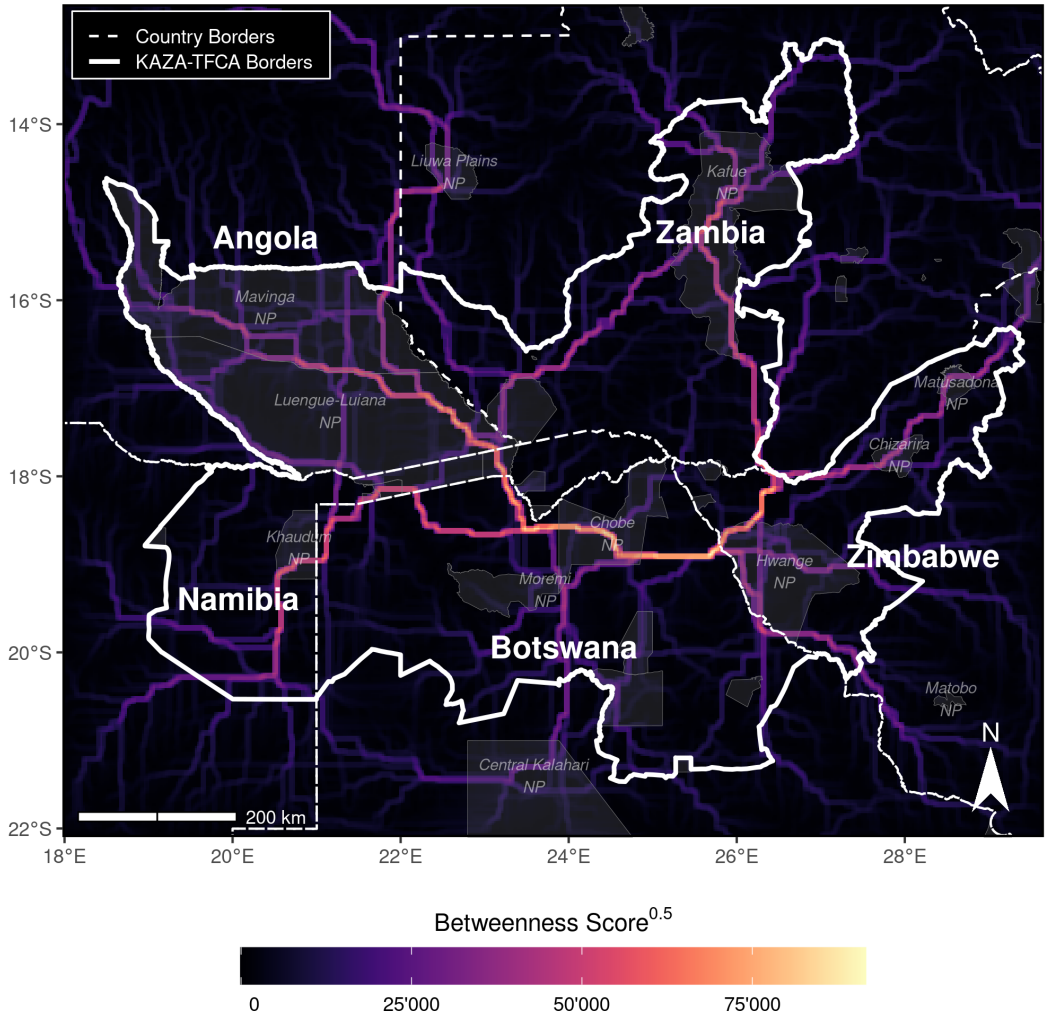


**Figure 5:** Map of betweenness scores, highlighting distinct dispersal corridors and potential bottlenecks across the extent of the KAZA-TFCA. Betweenness measures the number of shortest paths traversing through each node (raster-cell). Hence, a high betweenness score indicates that the respective area is exceptionally important for connecting different regions in the study area. The metric is therefore useful to pinpoint discrete movement corridors (Bastille-Rousseau et al., 2018). Note that we square-rooted betweenness scores to improve visibility of corridors with comparably low scores. Additional betweenness maps showing betweenness scores when individuals move fewer than 2'000 steps are provided in Figure S6.

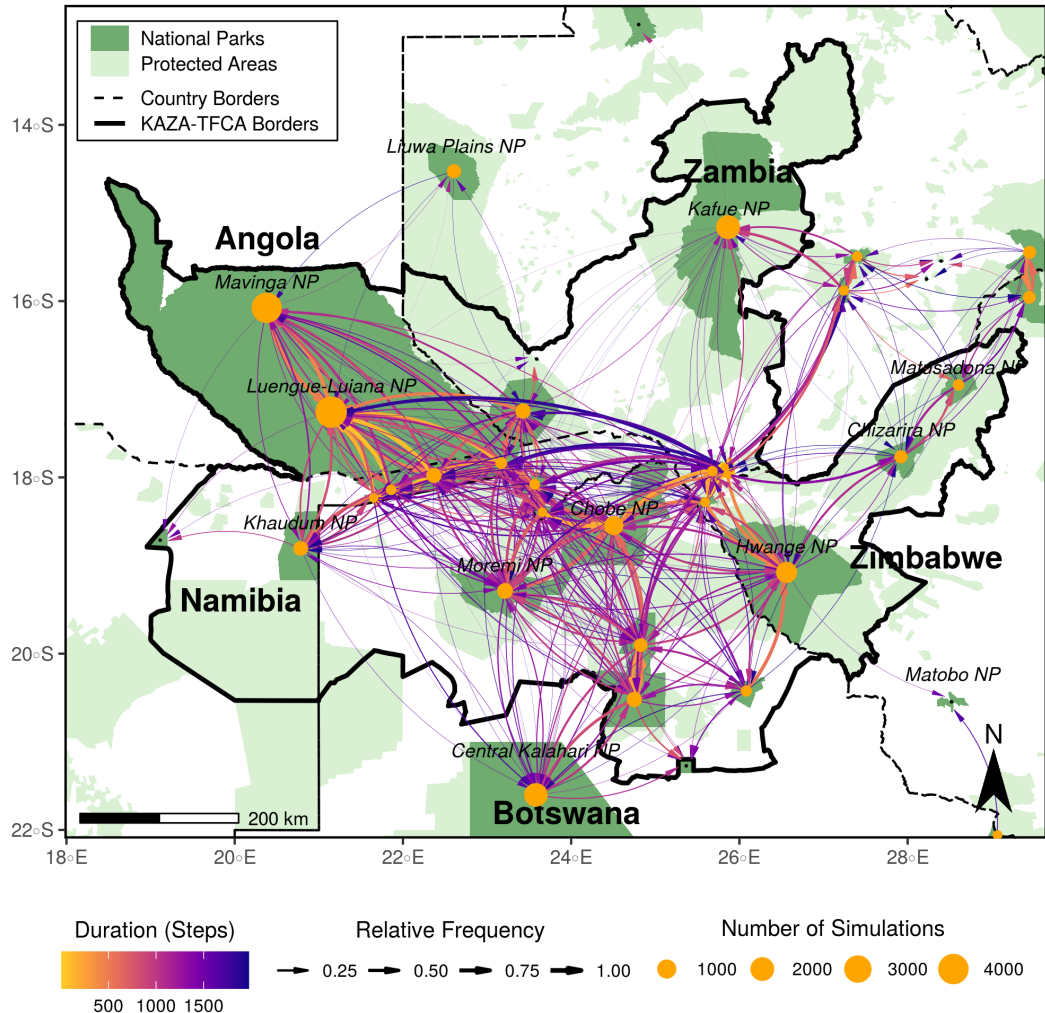


**Figure 6:** Map of inter-patch connectivity in relation to dispersal duration, highlighting connections between NPs (dark green). Yellow bubbles represent the center of the different NPs and are sized in relation to the number of simulated dispersers originating from each park. Black dots represent NPs that were smaller than  $700 \text{ km}^2$  and therefore were not used as source areas. Arrows between NPs illustrate between which NPs the simulated dispersers successfully moved and the color of each arrow shows the average number of steps (i.e. 4-hourly movements) that were necessary to realize those connections. Additionally, the line thickness indicates the relative number of dispersers originating from a NP that realized those connections.